Robotic Disease Detection in Greenhouses: Combined Detection of Powdery Mildew and Tomato Spotted Wilt Virus

Noa Schor, Avital Bechar, *Member, IEEE*, Timea Ignat, Aviv Dombrovsky, Yigal Elad, and Sigal Berman, *Member, IEEE*

***Abstract*—Robotic systems for disease detection in greenhouses are expected to improve disease control, increase yield, and reduce pesticide application. We present a robotic detection system for combined detection of two major threats of greenhouse bell peppers: Powdery mildew (PM) and *Tomato spotted wilt virus* (TSWV). The system is based on a manipulator, which facilitates reaching multiple detection poses. Several detection algorithms are developed based on principal component analysis (PCA) and the coefficient of variation (CV). Tests ascertain the system can successfully detect the plant and reach the detection pose required for PM (along the side of the plant), yet it has difficulties in reaching the TSWV detection pose (above the plant). Increasing manipulator work–volume is expected to solve this issue. For TSWV, PCA-based classification with leaf vein removal, achieved the highest classification accuracy (90%) while the accuracy of the CV methods was also high (85% and 87%). For PM, PCA-based pixel-level classification was high (95.2%) while leaf condition classification accuracy was low (64.3%) since it was determined based on the upper side of the leaf while disease symptoms start on its lower side. Exposure of the lower side of the leaf during detection is expected to improve PM condition detection.**

***Index Terms*—Agricultural automation, computer vision for automation.**

I. Introduction

GREENHOUSE conditions are controlled to maximize production and plant growth rate. Such conditions are also favorable for the spread of fungal, bacterial, and viral diseases as well as theirs vectors. Consequently periodic and repetitive disease detection and monitoring during plant lifecycle, from transplanting to harvesting, is essential for reaching full production potential and for preventing significant yield losses [1], [2]. Early detection is crucial for ensuring successful disease containment following application of appropriate counter measures. Improving disease detection procedures is a critical facet in increasing greenhouse productivity, quality, and sustainability.

To-date, disease detection and monitoring in greenhouses are conducted manually by experts and are limited due to human resources availability, low sampling rate, and high monitoring costs. An inspector examines the flora for symptoms while traversing the greenhouse rows on foot. A sample of plants is inspected in several locations determined arbitrarily according to experience, typically, in a fixed pattern (the same locations are revisited and sampled in all plots). Sampling resolution tends to be low with about 20 locations sampled per hectare and each plot is monitored every 7–10 days. The inspector walks about 20 km per day covering about 8 hectares. Therefore, a dedicated inspector is required for every 70–80 hectares. The limitations of the current inspection methods can lead to late detection of an incipient infection and consequently to inability to contain the disease. As a precaution, repeated, high doses of pesticide are often implemented even when symptoms are far below thresholds which mandate pesticide application. Moreover pesticides are typically applied uniformly throughout the greenhouse while disease distribution is typically centered in distinct locations.

Automation of disease detection and monitoring can facilitate targeted and timely disease control which can lead to increased yield, improved crop quality, and massive reduction in the quantity of applied pesticides. These in turn can lead to reduced production costs, reduced exposure to pesticides of farm workers and inspectors, and increased sustainability. Albeit the clear benefits, robotics systems for disease detection and monitoring are currently not available on the market since their development is very challenging. The plant growth process is only partly controlled and each disease has different symptoms and different progression characteristics in different cultivars (color, pattern, growth region, etc.), mandating unique detection procedures for each disease and cultivar. In recent years, new pesticide application regulations, along with the growing competition in the high-value crop market are driving investments in development of disease detection and monitoring technology.

Manuscript received August 31, 2015; accepted December 31, 2015. Date of publication January 14, 2016; date of current version February 12, 2016. This paper was recommended for publication by Associate Editor J. Kim and Editor W. Kyun Chung upon evaluation of the reviewers' comments. This work was supported by the Chief Scientist Fund of the Ministry of Agriculture under Grant 459-4450-12. The work of S. Berman and N. Schor was supported by the Helmsley Charitable Trust through the Agricultural, Biological, and Cognitive Robotics Initiative of Ben-Gurion University of the Negev.

N. Schor is with the Department of Industrial Engineering and Management, Ben-Gurion University of the Negev, Beer-Sheva 84105, Israel, and also with the Institute of Agricultural Engineering, Agricultural Research Organization, Beit Dagan 50250, Israel (e-mail: noasch@bgu.ac.il).

A. Bechar and T. Ignat are with the Institute of Agricultural Engineering, Agricultural Research Organization, Beit Dagan 50250, Israel (e-mail: avital@volcani.agri.gov.il).

A. Dombrovsky and Y. Elad are with the Institute of Plant Protection, Agricultural Research Organization, Beit Dagan 50250, Israel (e-mail: aviv@volcani.agri.gov.il).

S. Berman is with the Department of Industrial Engineering and Management, Ben-Gurion University of the Negev, Beer-Sheva 84105, Israel (e-mail: sigalbe@bgu.ac.il).

Digital Object Identifier 10.1109/LRA.2016.2518214

There is still very little research on the development of integrated robotic disease detection systems using proximal sensing techniques (where a camera is mounted on robot or a ground platform moving inside the plot), probably, as the preliminary challenge of development of robust disease detection algorithm for such conditions is still an open research question. Aerial platforms [3] and mobile robotic platforms with fixed sensor configurations [4], [5] for disease detection have been tested for open field crops. However, in greenhouses both solutions have inherent shortcomings. For aerial systems, maneuverability within greenhouses construction is limited depriving them of their main outdoor advantage. Fixed sensor configurations do not allow pose adaptation during run-time which is problematic due to greenhouse plant growth characteristics. Also, navigation and localization cannot rely on GPS sensors since the construction can cause unpredictable errors. In greenhouses pose adaptation can significantly improve detection especially early detection where symptoms spread is still minimal. Moreover in fixed configuration systems the requirement for multiple disease detection can lead to a requirement for multiple detection poses which tends to increase system complexity and cost and hinder maneuverability.

A mobile robotic manipulator carrying detection sensors can overcome these limitations. The manipulator facilitates multiple detection poses and run-time adaptability along with fast operation cycle times. Due to these traits robotic manipulators are commonly used for fault detection tasks in industry [6]. Mobile platforms offer required maneuverability within the greenhouse isles and are commonly used in greenhouses for a variety of tasks (e.g., spraying [7] and harvesting [8]). To-date development of a mobile-manipulator based disease detection system has not been reported, probably since researchers have not yet confronted the automation of the detection of multiple greenhouse diseases. To the best of our knowledge, the current research is the first to develop a greenhouse disease detection system for multiple diseases and thus the first to develop a disease detection system based on the concept of a mobile manipulator.

Development of a robust disease detection apparatus suitable for mobile manipulators is a major challenge in system development. The apparatus must be developed for the environment (greenhouse), the system (mobile manipulator), the specific cultivar, and for the characteristics of the symptoms of the plant's diseases. Optical-based sensors for disease detection have many advantages, as they offer non-destructive and fast detection capabilities along with low weight and dimensions and thus simple system integration [9]. Researchers have applied image processing techniques to detect, quantify, and classify various plant diseases in many different cultivars (for reviews see [10]–[12]). Various classification methods have been used, e.g., principal component analysis (PCA) [13], [14], neural networks [4], and support vector machines [15]. Plant diseases can affect various optical foliage characteristics therefore disease detection can be based on different spectral ranges [16] such near infra-red (NIR) spectrum [4] and visible spectrum [17]. The current research is the first to developed image-based detection algorithms for TSWV and the first to tackle PM detection in peppers. The developed algorithms adhere to the requirements of integration with the developed robotic disease detection system.

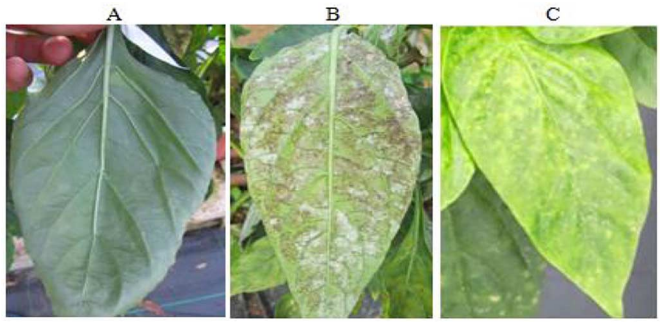

Fig. 1. Pepper leaves. A. Healthy; B. Powdery mildew; C. *Tomato spotted wilt virus*.

Bell pepper (*Capsicum annuum*) is a specialty, high-value crop, grown mostly in greenhouses for fresh markets. It is cultivated worldwide and used as food ingredient, spice, and as an ingredient in medicine. Two common threats of greenhouse pepper plants are the Powdery mildew (PM) fungi and the *Tomato spotted wilt virus* (TSWV) [2]. These threats have severe consequences to both fruit and plant and both are the most damaging in their respective category (fungi and viral). Detection of these threats during a single pass of a robotic system is challenging as their characteristics differ in visible symptoms and in outbreak regions.

PM [Fig. 1(B)], caused by the fungus *Leveillula taurica*, is a serious threat to greenhouse pepper production [18]. Leaves infected by PM shed prematurely, resulting in a reduced photosynthetic area, inhibition of fruit development, reduction in the number of flowers per plant, and increased sunburn damage to exposed fruit [1], [19]. Heavy epidemics of PM can cause a significant yield loss, i.e., two-four kg/m^2 [20]. The visible symptoms of PM in peppers are yellow-brown spots with whitish powdery mycelium which typically appear first on the underside of older, lower leaves [2].

TSWV [Fig. 1(C)] is transmitted by eight species of thrips (e.g., western flower thrips *Frankliniella occidentalis*) [2] in a persistent and propagative manner [21]. The disease is considered a major threat in many vegetable production areas. In pepper plants, TSWV causes a range of symptoms: sudden yellowing, mild mottling, mosaic, browning of young leaves on the upper part of the plant which later become necrotic, and occasionally ring-shaped spots which appear on both leaves and fruits. TSWV causes heavy crop losses since fruit formed after infection display large necrotic streaks and spots while younger fruit may become totally necrotic [22]. Early detection of TSWV in pepper plants is crucial as it has only recently migrated to peppers overcoming plant resistance [23]. Currently there is no appropriate treatment for TSWV in peppers, and thus infected plants must be eradicated and destroyed as soon as possible.

Early detection of TSWV has been studied using chemical sensors, e.g., ELISA (enzyme-linked immunosorbent assay) [23]. Such methods are destructive as leaves must be extracted and they are not suitable for application in the field during runtime. Moreover, due to the uneven distribution of TSWV in the

greenhouse, the selection of samples to be tested has a crucial influence on detection reliability. Therefore image-based detection developed in the current work has multiple advantages over the existing methods. Imaged-based detection algorithms have been developed for PM in grapevine [24], [25] and wheat [26] using UV [24] and multispectral cameras [25], [26]. The developed UV-based detection method requires complex fluorescents excitation, and its implementation outside the laboratory has not been demonstrated. The visible light spectrum used in the current work is much simpler and can avoid the high costs of fluorescence or multispectral imaging systems, which can be prohibiting for deployment in small and medium farms, which is often the case for greenhouse operation. Moreover, visible light based detection of both PM and TSWV was found superior to NIR-based detection [13].

We are developing a robotic disease detection system, based on a manipulator, for the two main threats of greenhouse peppers: PM and TSWV. System components (system architecture, end effector and sensing apparatus, operation cycle, and detection algorithms) are developed in a holistic manner, as integration of perception requirements in early stages of system development is important in agricultural environments where both task and environment characteristics are very challenging [27]. The overall concepts and technical design of the system have been presented in [28]. The current letter presents the development of the system's architecture and operation cycle along with the development of disease detection algorithms based on the visual spectrum. The rest of this letter is organized as follows: section II presents the system architecture and operation cycle; section III presents the developed disease detection algorithms, finally a discussion is presented in section IV.

II. System Architecture

A. Method

The robotic disease detection system for greenhouse peppers [28] includes three main components: a robotic manipulator, a custom-made end-effector, and a sensory apparatus (Fig. 2). The sensory apparatus comprises an RGB camera and a laser sensor (DT35, SICK). The sensors are aligned in parallel and are mounted on the end-effector which is attached to a 6 degrees-of-freedom (DoF) industrial manipulator (MH5L, Motoman, Japan).

The robotic manipulator is currently situated near a conveyor belt carrying pots with plants, simulating the movement of the robotic platform in a greenhouse plot. It will later be mounted on a mobile platform that will drive through the greenhouse aisle. Plant canopy is identified using blob analysis based on RGB images. Upper and lower bounds on the RGB values of leaves were pre-calculated based on 20 leaves. These thresholds are used for transforming the color image to a binary image and binary filters are used for region growing and smoothing. The canopy is identified as the largest blob in the binary image [28]. Once a plant is identified, the disease detection procedure is initiated. To facilitate the required rapid operation, enabling high sampling resolution and large area coverage, disease detection is done during a single pass of the robot manipulator about the plant while the conveyer (or mobile platform) is in motion. To further shorten operation cycle time, TSWV detection is done first since if TSWV is detected the plant is marked for eradication, thus detection of PM for the same plant is not required.

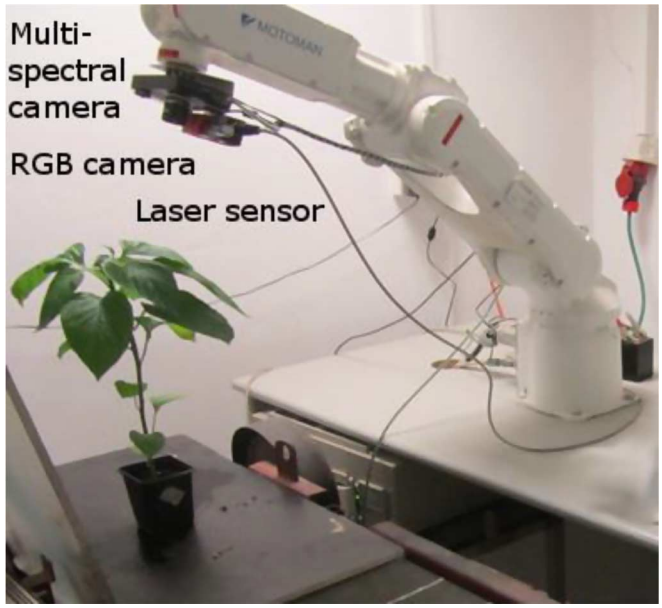

Fig. 2. The robotic disease detection system: a manipulator, a custom-made end-effector with an RGB camera and a laser sensor. The apparatus currently additionally includes a multispectral camera (NIR, red, and green) yet tests showed the superiority of RGB over NIR-based detection [13].

Based on the results of the blob analysis and the kinematic model of the system, the plant location with respect to the robot is calculated. The robot is positioned at a detection pose above the plant (sensor apparatus facing down) at an a-priori determined distance from the plant foliage which facilitates required leaf resolution. During the motion towards the detection pose the laser sensor is sampled. The robot corrects the final pose based on the smallest sampled distance. TSWV detection is executed and in case of a negative result the robot is repositioned alongside the plant based on canopy detection from the side (sensor apparatus facing sideways towards the plant). Once again the laser sensor is used for fine-tuning the distance from the plant. From this pose PM detection is conducted. When the manipulator moves from the TSWV detection pose to the PM detection pose it may collide with the plant. Such collisions are problematic even when there is no visible damage to the plant as any contact with the system can potentially transmit infections between plants. To avoid this, the manipulator moves through an intermediate-point designed to secure motion outside the plant foliage [28].

B. Operation Cycle Tests

The system's operation cycle was tested in an indoor laboratory environment (Fig. 2). Three different plant locations (770, 900 and 1050 mm away from the robotic system base in workspace coordinate) and three end-effector velocities (5, 15 and 25 mm/sec) were tested to examine the suitability of

the robotic workspace and motion profiles, and for ascertaining system capability of attaining required detection poses. Each condition was repeated using 10 healthy plants (90 runs).

Collisions of the robot with the plant were examined along with two measures of the system's ability of attaining the required detection poses: plant identification rate, which was defined as the percent of correctly identified plants (from each approach direction); and correct camera positioning rate which was defined as the number of times the camera was correctly positioned for detection divided by the number of correctly identified plants (for each detection pose). Correct positioning of the camera is defined when the center of the image is inside the plant canopy bounding square.

Collisions were observed only in five out of the 30 trials for plants located 770 mm from the robotic system base (there were no collisions for the other conditions). Two collisions occurred when the manipulator moved from the TSWV detection pose (above the plant) to the intermediate point, and three collisions occurred when the manipulator moved from the intermediate point to the PM detection pose (alongside the plant). For the PM detection pose, plant identification rate was high for all plant locations (770 mm: 90%, 900 mm: 96%, 1050 mm: 93%, average: 93%). For the TSWV detection pose, plant identification rate (average: 83%) was high for close and medium distance plants (770 mm: 100% and 900 mm: 90%), whereas for remote plants it was low (1050 mm: 60%). Correct camera positioning rate was high for the PM detection pose (770 mm: 81%, 900 mm: 86%, 1050 mm: 82%, average: 83%) while it was low for the TSWV detection pose (770 mm: 47%, 900 mm: 33%, 1050 mm: 17%, average: 32%).

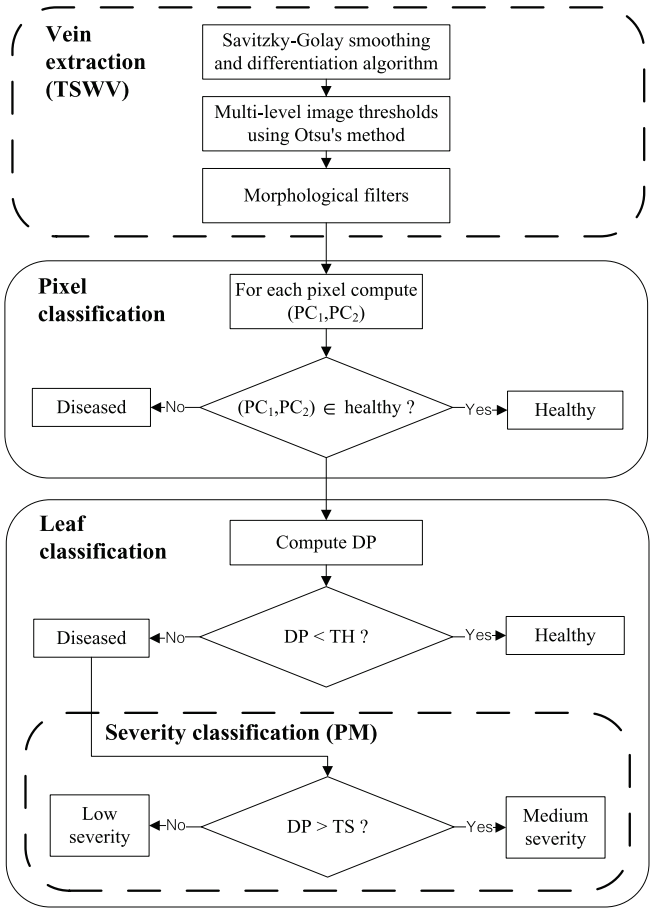

Fig. 3. PCA-based detection algorithm. DP: ratio of diseased pixels, TH: healthy threshold, TS: severity threshold.

III. Disease Detection

A. Method

Each detection algorithm starts with leaf segmentation and removal of background noise based on blob analysis and morphological filters. For PM the developed detection algorithm is based on PCA (Fig. 3). As this is the first research targeting TSWV detection, three different detection algorithms were developed and compared: a PCA-based algorithm (Fig. 3) and two algorithm variants based on the coefficient of variation (CV) [29] (Fig. 4).

1) Principal Component Analysis for PM: For PM, there is a high contrast between disease symptoms and leaf color [Fig. 1(B)], therefore a classification algorithm was developed based on the RGB channels. Each leaf pixel is classified as healthy or diseased based on the first two principal components of the pixel's RGB values [13]. The leaf is than classified as healthy, diseased low severity, or diseased medium severity based on the ratio of diseased pixels (DP). The severity differentiation is required for treatment planning.

2) Principal Component Analysis for TSWV: For TSWV, the contrast of the symptom color and leaf color is mild and leaf veins and disease symptoms have similar colors [Fig. 1(C)], thus for color based detection of TSWV it is imperative that the leaf veins are first extracted. A leaf vein extraction algorithm was implemented using Savitzky-Golay smoothing and differentiation algorithm [30] followed by multi-level image thresholds using Otsu's method [31] and morphological filters (e.g. area open and dilate). Following the leaf vein extraction, each leaf pixel is classified as healthy or diseased based on the first two principal components of the pixel's RGB values [13]. The leaf is than classified as healthy or diseased based on the

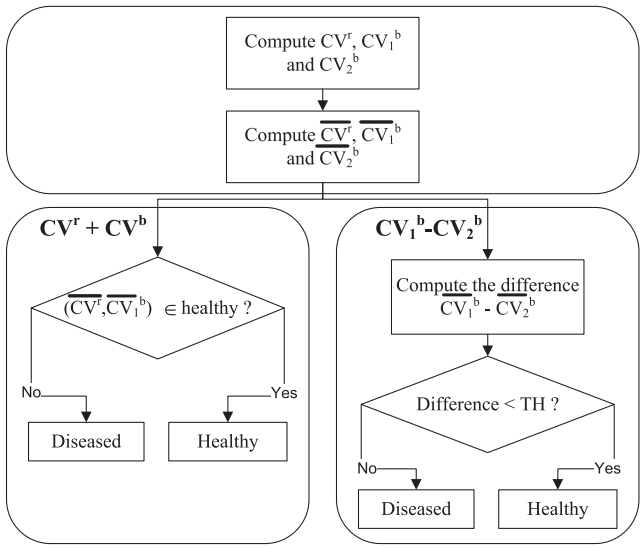

Fig. 4. CV-based TSWV detection algorithms. TH: healthy threshold.

ratio of diseased pixels (DP). Disease severity is not determined since plant eradication is required even if severity is low.

3) Coefficient of Variation of TSWV Symptom Pattern: Since TSWV symptoms are characterized by a mosaic pattern, classification based on the coefficient of variation (CV) was explored (Fig. 4). The CV of a moving window is calculated for each RGB channel (red: CV^{r}, green: CV^{g}, and blue: CV^{b}) by dividing the standard deviation of the color value by its mean within the window. The leaf is scanned right-to left, and top-down, were at each step the window is advanced by a single pixel. Different window sizes for all three colors were visually examined and two decision rules were implemented based on the examination: $\mathrm{CV}^{\mathrm{r}}+\mathrm{CV}^{\mathrm{b}}$ in which the classification decision is based on the values of the average red channel CV ($\overline{CV^r}$) and the average blue channel CV ($\overline{CV^b}$) of the same window size; and $\overline{CV_1{}^b}-\overline{CV_2{}^b}$ in which the classification decision is based on the difference between two $\overline{CV^b}$values from two window sizes ($\overline{CV_1{}^b}-\overline{CV_2{}^b}$, where window 1 is larger than window 2).

B. Experiment

1) Database Construction: Plants of sweet pepper (Hazera Genetics) were obtained from a commercial nursery (Hishtil, Ashkelon, Israel) 40–50 days after seeding and were transplanted into 36 pots containing soil and potting medium. Plants were fertigated proportionally with drippers 2–3 times per day with 5:3:8 NPK fertilizer (nitrogen (N), phosphorus (P) and potassium (K)), allowing for 25–50% drainage. Irrigation water was planned to have total N, P and K concentrations of 120, 30 and 150 mg/L, respectively; electrical conductivity of water (EC) was 2.2 dS/m. Plants were maintained at 20 to 30°C in a pest and disease free greenhouse where their healthy status was ascertained by visual inspections of a plant pathologist.

The 36 plants were divided into two subsets: 24 plants for PM detection and 12 plants for TSWV detection. Each subset was positioned in a different greenhouse. All the images were acquired in the greenhouse during noon time. The images were acquired with an RGB camera (PowerShot SX210 IS, Canon, USA) with a resolution of 4320×3240 pixels. For the PM subset, four months after transplant 12 out of 24 plants were infected with PM. Starting at the visual appearance of the first symptom (two days after infection), images of both sides of 24 selected leaves (12 healthy and 12 diseased) each from a different plant were acquired every three days over a 17 day period. Three leaves (two healthy and one diseased) were torn unintentionally during data collection and their images were discarded. For the TSWV subset, two-weeks after transplant 6 out of 12 plants were infected with TSWV. Three days after infection, images of the top and sides of the plants were taken daily for 15 consecutive days (days 3 to 17 after infection). Images of plants rather than leaves were taken as the plants were small. For both diseases, in addition to disease intensity, the images convey pigmentation due to possible interfering nutritional or physiological disorders.

TSWV and PM symptoms in all images were manually marked by a plant pathology expert [28]. The pathologist additionally classified the condition of each leaf on every recorded day. Leaves were classified as either healthy or diseased and disease severity was additionally graded as low, medium, or high. For leaf classification in the PM database the pathologist used the images of both sides of the leaf. For the TSWV database leaf classification was done using the images of the top of the plant.

2) Environment: Image analysis was conducted using a computer equipped with an Intel i7-3632QM 2.2 GHz processor with turbo boost up to 3.2 GHz (CPU) and 8 GB RAM with a Windows 8 (64-bit) operating system. The detection algorithms were implemented using Matlab (Mathworks, USA), and statistical analysis was conducted using IBM SPSS statistics (IBM, USA).

3) Parameter Determination: For PCA-based algorithms, pixel level classification thresholds were computed based on the analysis of a healthy leaf and a diseased leaf (a leaf infected with PM or a leaf infected with TSWV after leaf vein removal). The threshold was determined after examination of separation using linear discriminant analysis (LDA) and using quadratic discriminant analysis (QDA). The function that offered improved separation was selected. Leaf classification thresholds based on DP were empirically determined for each disease based on visualization of DP results for healthy and diseased leaves with a box plot graph.

For CV-based algorithms, the average and standard deviation of CV of each color channel (RGB) in different window sizes (5×5 *to* 135×135 pixels) was calculated for 24 sample images (12 of healthy leaves and 12 of infected leaves). Window sizes for both algorithm variants were chosen based on examination of specificity values and run-time. Specificity reflects the ratio of infected plants which the algorithm correctly recognizes [29]:

$$specificity = \frac{TN}{TN + FP} \tag{1}$$

where healthy is regarded as positive and diseased is regarding as negative. FP is false positive, and TN is true negative. Specificity is used rather than accuracy since for TSWV high identification rate of infected plants is critical. For the CV^{r} + CV^{b} algorithm, the region of the healthy class was determined using LDA or QDA. For the $\mathrm{CV}_1{}^b$–$\mathrm{CV}_2{}^b$ algorithm, the decision threshold was empirically determined using a box plot graph.

4) Analysis: Leaf classification quality was determined based on 10×2 cross validation. Results are presented using confusion matrixes along with overall accuracy which reflects the ratio of correct classification (both healthy and diseased):

$$accuracy = \frac{TP + TN}{TP + FP + FN + FN} \tag{2}$$

where TP is true positive and FN is false negative.

C. Results

1) PM Detection: A total of 45 images were analyzed from the PM data base: 15 images of healthy leaves, 11 images of leaves with low severity symptoms and 19 images of leaves

TABLE I
CONFUSION MATRIX—PM LEAF CLASSIFICATION

		Actual		
		Healthy mean (STD)	*Low severity mean (STD)*	*Medium severity mean (STD)*
Predicted	*Healthy*	71.2% (18.0%)	35.8% (10.7%)	15.5% (5.4%)
	Low severity	27.4% (17.1%)	45.3% (18.2%)	8.2% (8.1%)
	Medium severity	1.4% (4.3%)	18.9% (15.4%)	76.3% (11.1%)
Average number of leaves		7.3	5.3	9.7

TABLE II
CONFUSION MATRIX—TSWV LEAF CLASSIFICATION

			Actual	
			Healthy mean (STD)	*Diseased mean (STD)*
Predicted	*PCA-based*	*Healthy*	89.4% (6.7%)	9.3% (5.6%)
		Diseased	10.6% (6.7%)	90.7% (5.6%)
	CV^r+ CV^b window size 35x35	*Healthy*	91.1% (5.4%)	24.0% (11.8%)
		Diseased	8.9% (5.4%)	76.0% (11.8%)
	CV_1^b-CV_2^b window sizes 25x25 and 5x5	*Healthy*	85.0% (5.3%)	10.0% (5.7%)
		Diseased	15.0% (5.3%)	90.0% (5.7%)
Average number of leaves			18.0	15.0

with medium severity. All analyzed images were of the upper side of the leaf which is naturally visible and from which the robotic system is planned to acquire images for PM detection. The average leaf classification confusion matrix is presented in Table I.

For PCA-based pixel level classification QDA was selected as it offered improved separation (95.2%) with respect to LDA (94.8%). For leaf classification, the healthy average classification threshold was TH $= 0.08$, and the average severity classification threshold was TS $= 0.2$. The average leaf classification accuracy was 64.3%.

2) TSWV Detection: A total of 72 images were analyzed from the TSWV database: 36 images of healthy and 36 images of infected plants. The visible symptoms of TSWV appear about 12 days after infection and at the 17th day the symptoms were in general clearly visible. Accordingly, analyzed images of infected plants were taken from plants with leaves marked as having low and medium severity of TSWV (18 low, 12 medium) 12 to 17 days after infection. Analyzed images of healthy leaves were taken from day-matched leaves. Images of three infected plants taken 12 days after infection were excluded because visible symptoms had not yet appeared, and three images taken 14, 15, or 16 days after infection were excluded due to pathologist detection errors. TSWV symptoms usually appear at the top of the plant, therefore all analyzed images were taken from the top view. Visual inspection verified that TSWV symptoms were indeed undetectable from the side view. The average leaf classification confusion matrixes for all algorithms are presented in Table II.

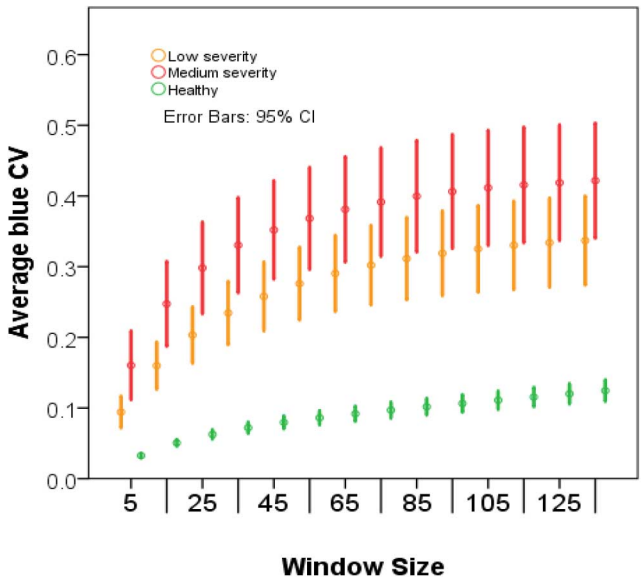

Fig. 5. $\overline{CV^b}$ distribution in different window sizes for 12 images of healthy leaves and 12 images of infected leaves. CI: confidence interval.

For PCA-based pixel level classification QDA was selected as it offered improved separation (85.6%) with respect to LDA (83.5%). For leaf classification, the average classification threshold was TH $= 0.34$. The average leaf classification accuracy was 90%.

For average CV calculation, smaller windows incurred shorter run times while larger windows had better specificity, yet run time increased with window size faster than specificity. For example, for a 35×35 window size the average run time for a sample of four leafs was 40 sec while the specificity was 80%. For a 125×125 window size the average run time was 56 sec and specificity was 83%. Therefore, a window size of 35×35 was chosen for $\mathrm{CV^r} + \mathrm{CV^b}$ classification. QDA was selected as it outperformed LDA. Average accuracy of leaf classification was 84%.

Visual examination shows that $\overline{CV^b}$values increase in diseased leaves faster than in healthy leaves especially for lower window size (Fig. 5). Therefore, $\mathrm{CV_1^b} - \mathrm{CV_2^b}$ classification was done with window sizes of 25×25 (large window) and 5×5 (small window). The average classification threshold was TH $= 0.0493$. The average leaf classification accuracy was 87%.

IV. DISCUSSION

In the operation cycle tests, all collisions occurred when the manipulator moved to and from the intermediate-point for close plants. This suggests that the intermediate-point should be redefined or be dynamically adjusted according the plant distance. For PM, results ascertain system capability of attaining the required detection pose. For TSWV, results indicate that the system has difficulty in successfully positioning the sensor apparatus and attaining the required detection pose. Increasing the robotic work-volume, e.g., by using a longer arm will be examined.

High accuracy was obtained for PM detection at the pixel level (95%) using PCA-based classification. However, while correct detection of healthy leaves (71%) or leaves with medium severity (76%) was high, correct detection of leaves with low severity was very low (45%) making the overall classification accuracy of leaf condition low (64%). This is caused since PM symptoms start appearing on the lower side of the leaf while the analyzed images were taken from the upper side of the leaf which is naturally more visible. The results clearly demonstrate that for early detection, the lower side of the leaf must be inspected. Thus a subsystem facilitating "in-to" the canopy sensing and exposure of the lower side of the leaf, e.g., an air blower along with a fast camera, is required.

For TSWV leaf classification, the accuracy of the PCA-based classification algorithm (90%) was highest. Classification based on CV was also high ($\mathrm{CV^r} + \mathrm{CV^b} : 84\%$ and $\mathrm{CV_1^b} - \mathrm{CV_2^b} : 87\%$). These results ascertain that TSWV can indeed be identified by images taken from above the plant. Results additionally show that TSWV cannot be identified from images taken from the side of the plant and thus two detection poses are required for a system identifying both diseases (PM from the side and TSWV from above) as anticipated. For the CV-based methods, correct identification of healthy leaves is high for the $\mathrm{CV^r} + \mathrm{CV^b}$ method (91%) while correct identification of infected leaves is high for the $\mathrm{CV_1^b} - \mathrm{CV_2^b}$ method (90%). Therefore integration of these two methods may lead to higher detection accuracy. CV-based algorithms may have an advantage over PCA-based algorithms in varying lighting conditions; therefore, both algorithms should be further tested in field experiments.

ACKNOWLEDGMENT

The authors would like to thank Dalia Rav-David, Oded Lachman, and Yossi Portal for ensuring the healthy status of pepper plants and the normal disease development.

REFERENCES

[1] Y. Elad, Y. Messika, M. Brand, D. Rav David, and A. Sztejnberg, "Effect of microclimate on Leveillula taurica Powdery mildew of sweet pepper," *Phytopathology*, vol. 97, no. 7, pp. 813–824, Jul. 2007.

[2] K. L. Pernezny, P. D. Roberts, J. F. Murphy, and N. P. Goldberg, *Compendium of Pepper Diseases*. Menasha, WI, USA: American Phytopathological Soc., 2003, ch. 1.

[3] S. F. Gennaro *et al.*, "An UAV-based remote sensing approach for the detection of spatial distribution and development of a grapevine trunk disease," in *Proc. 8th Int. Workshop Grapevine Trunk Dis.*, Spain, 2012, pp. 734–737.

[4] D. Moshou *et al.*, "Intelligent multi-sensor system for the detection and treatment of fungal diseases in arable crops," *Biosyst. Eng.*, vol. 108, no. 4, pp. 311–321, Apr. 2011.

[5] S. K. Pilli, B. Nallathambi, S. J. George, and V. Diwanji, "eAGROBOT—A robot for early crop disease detection using image processing," in *Proc. IEEE Int. Conf. Electron. Commun. Syst.*, India, Feb. 13–14, 2014, pp. 1–6.

[6] M. P. Groover, M. Weiss, R. N. Nagel, and N. G. Odrey, *Industrial Robotics: Technology, Programming, and Applications*. New York, NY, USA: McGraw-Hill, 1986.

[7] R. Gonzalez, F. Rodriguez, J. Sanchez-Hermosilla, and J. G. Donaire, "Navigation techniques for mobile robots in greenhouses," *Appl. Eng. Agric.*, vol. 25, no. 2, pp. 153–165, Mar. 2009.

[8] E. J. Van Henten *et al.*, "An autonomous robot for harvesting cucumbers in greenhouses," *Auton. Robots*, vol. 13, no. 3, pp. 241–258, Nov. 2002.

[9] S. Sankaran, A. Mishra, R. Ehsani, and C. Davis, "A review of advanced techniques for detecting plant diseases," *Comput. Electron. Agric.*, vol. 72, no. 1, pp. 1–13, Jun. 2010.

[10] A. Barbedo and J. Garcia, "Digital image processing techniques for detecting, quantifying and classifying plant diseases," *SpringerPlus*, vol. 2, p. 660, Dec. 2013.

[11] J. D. Pujari, R. Yakkundimath, and A. S. Byadgi, "Image processing based detection of fungal diseases in plants," in *Proc. Int. Conf. Inform. Commun. Technol.*, India, 2015, pp. 1802–1808.

[12] J. K. Patil and R. Kumar, "Advances in image processing for detection of plant diseases," *J. Adv. Bioinformat. Appl. Res.*, vol. 2, no. 2, pp. 135–141, Jun. 2011.

[13] N. Schor, S. Berman, A. Dombrovsky, Y. Elad, T. Ignat, and A. Bechar, "Perception apparatus design for a robotic system for greenhouse pepper disease detection," *Precision Agriculture*, 2016, to be published.

[14] L. Bagnasco, M. Zotti, N. Sitta, and P. Oliveri, "A PCA-based hyperspectral approach to detect infections by mycophilic fungi on dried porcini mushrooms (boletus edulis and allied species)," *Talanta*, vol. 144, pp. 1225–1230, Nov. 2015.

[15] T. Rumpf, A. K. Mahlein, U. Steiner, E. C. Oerke, H. W. Dehne, and L. Plümer, "Early detection and classification of plant diseases with support vector machines based on hyperspectral reflectance," *Comput. Electron. Agric.*, vol. 74, no. 1, pp. 91–99, Oct. 2010.

[16] W. S. Lee, V. Alchanatis, C. Yang, M. Hirafuji, D. Moshou, and C. Li, "Sensing technologies for precision specialty crop production," *Comput. Electron. Agric.*, vol. 74, no. 1, pp. 2–33, Oct. 2010.

[17] V. Tajane and N.J. Janwe, "Medicinal plants disease identification using canny edge detection algorithm, histogram analysis and CBIR," *Int. J. Adv. Res. Comput. Sci. Softw. Eng.*, vol. 4, no. 6, pp. 530–536, Jun. 2014.

[18] Z. Zheng *et al.*, "Loss of function in mlo orthologues reduces susceptibility of pepper and tomato to Powdery mildew disease caused by Leveillula taurica," *PLoS ONE*, vol. 8, no. 7: e70723, Jul. 2013. doi: 10.1371/journal.pone.0070723

[19] R. Smith, S. T. Koike, M. Davis, K. Subbarao, and F. Laemmlen, "Several fungicides control powdery mildew in peppers," *California Agric.*, vol. 53, no. 6, pp. 40–43, Nov. 1999

[20] R. F. Cerkauskas and A. Buonassisi, "First report of powdery mildew of greenhouse pepper caused by Leveillula taurica in British Columbia, Canada," *Plant Dis.*, vol. 87, no. 9, p. 1151, 2003.

[21] A. Fereres and B. Raccah, "Plant virus transmission by insects," eLS 1–12, Apr. 2015.

[22] Y. Avila, J. Stavisky, S. Hague, J. Funderburk, S. Reitz, and T. Momol, "Evaluation of frankliniella bispinosa (Thysanoptera: Thripidae) as a vector of the tomato spotted wilt virus in pepper," *Fla. Entomol.*, vol. 89, no. 2, pp. 204–207, Jun. 2006.

[23] A. Crescenzi, A. Viggiano, and A. Fanigliulo, "Resistance breaking tomato spotted wilt virus isolates on resistant pepper varieties in Italy," *Commun. Agric. Appl. Biol. Sci.*, vol. 78, no. 3, pp. 609–612, 2013.

[24] M. C. Belanger, J. M. Roger, P. Cartolaro, A. A. Viau, and V. Bellon-Maurel, "Detection of powdery mildew in grapevine using remotely sensed UV-induced fluorescence," *Int. J. Remote Sens.*, vol. 29, no. 6, pp. 1707–1724, Mar. 2008.

[25] R. Oberti, M. Marchi, P. Tirelli, A. Calcante, M. Iriti, and A. N. Borghese, "Automatic detection of powdery mildew on grapevine leaves by image analysis: optimal view-angle range to increase the sensitivity," *Comput. Electron. Agric.*, vol. 104, pp. 1–8, Jun. 2014.

[26] J. Franke and G. Menz, "Multi-temporal wheat disease detection by multi-spectral remote sensing," *Precis. Agric.*, vol. 8, no. 3, pp. 161–172, Jun. 2007.

[27] D. Eizicovits, B. Van Tuijl, S. Berman, and Y. Edan, "Integration of perception capabilities in gripper design using graspability maps," *Biosyst. Eng.*, available online January 13, 2016.

[28] N. Schor, S. Berman, A. Dombrovsky, Y. Elad, T. Ignat, and A. Bechar, "A robotic monitoring system for diseases of pepper in greenhouse," in *Proc. 10th Eur. Conf. Precis. Agric.*, Israel, 2015, pp. 627–634.

[29] B. S. Everitt and A. Skrondal, *The Cambridge Dictionary of Statistics*. Cambridge, U.K.: Cambridge Univ. Press, 1998.

[30] A. Savitzky and M. J. E. Golay, "Smoothing and differentiation of data by simplified least squares procedures," *Anal. Chem.*, vol. 36, no. 8, pp. 1627–1639, Jul. 1964.

[31] N. Otsu, "A threshold selection method from gray-level histograms," *IEEE Trans. Syst. Man Cybern.*, vol. 9, No. 1, pp. 62–66, Jan. 1979.